

How many interactions does it take to modify a jet?

Chiara Le Roux^a, José Guilherme Milhano^{b,c}, Korinna Zapp^a

^a*Dept. of Physics, Lund University, Sölvegatan 14A, S22362 Lund, Sweden*

^b*LIP, Avenida Prof. Gama Pinto, 2 P-1649-003 Lisboa, Portugal*

^c*Departamento de Física, Instituto Superior Técnico (IST), Universidade de Lisboa, Av. Rovisco Pais 1, P-1049-001 Lisboa, Portugal*

Abstract

It is a continued open question how there can be an azimuthal anisotropy of high p_{\perp} particles quantified by a sizable v_2 in p+Pb collisions when, at the same time, the nuclear modification factor R_{AA} is consistent with unity. We address this puzzle within the framework of the jet quenching model JEWEL. In the absence of reliable medium models for small collision systems we use the number of scatterings per parton times the squared Debye mass to characterise the strength of medium modifications. Working with a simple brick medium model we show that, for small systems and not too strong modifications, R_{AA} and v_2 approximately scale with this quantity. We find that a comparatively large number of scatterings is needed to generate measurable jet quenching. Our results indicate that the R_{AA} corresponding to the observed v_2 could fall within the experimental uncertainty. Thus, while there is currently no contradiction with the measurements, our results indicate that v_2 and R_{AA} go hand-in-hand. We also discuss departures from scaling, in particular, due to sizable inelastic energy loss.

1. Introduction

In the field of relativistic heavy ion collisions, the idea that high energy partons travelling through a medium will lose energy due to successive interactions with the medium constituents has long been established. This was done from the theoretical point of view [1, 2] (for reviews see [3–7]) and subsequently confirmed experimentally [8, 9] (for reviews see [10, 11]). The experimental confirmation was carried out via the measurement of nuclear modification factors, which compare the yields of high p_{\perp} particles or jets in heavy ion collisions to those in pp collisions, where no medium was expected to be formed. These measurements were then repeated in small collision systems such as d+Au and p+Pb and the absence of quenching was confirmed [12–23]. Such results motivated the interpretation of this suppression in the yields as a signature of the presence of a quark gluon plasma (QGP) phase in the early stages of relativistic heavy ion collisions.

As a means to investigate this newly discovered, short lived phase of matter, several other observables were proposed. One of them is the azimuthal momentum anisotropy, which is commonly characterised via the flow coefficients, v_n , appearing in the Fourier decomposition of the particle distribution

$$\frac{dN}{d\phi} = \frac{1}{2} \left(1 + 2 \sum_n v_n \cos(2(\phi - \Psi_n)) \right). \quad (1)$$

Here, Ψ_n is the azimuthal angle of the n^{th} symmetry plane. Since the overlap region of two colliding nuclei has a strong elliptical deformation, the corresponding elliptical term in the momentum distribution, v_2 , is the most prominent one

in heavy ion collisions. For $n = 2$, Ψ_2 is the orientation of the short axis of the overlap region. Therefore, when all $v_n = 0$, the distribution is completely isotropic and, as it acquires an ellipsoidal shape, a non-zero v_2 is observed.

Several experiments have measured the flow coefficients and found them to be non-zero in relativistic heavy ion collisions [24–28]. In these collisions a non-vanishing v_2 of low transverse momentum particles is a consequence of the collective flow of the system. Because the pressure gradient driving the expansion is larger along the short axis of the overlap region than along the long axis, the particles are pushed out preferentially along the short axis. At high p_{\perp} , v_2 is generated via the path length dependence of the energy loss suffered by the hard particle. It is thus also a consequence of the geometry of the system, but is not related to collective flow.

Surprisingly, sizable flow coefficients, in particular v_2 , were also observed in small systems [29, 30]. These systems are believed to be too short lived to develop collective flow, but it has been shown in kinetic theory that, even with a low number of scatterings per particle, a sizable soft particle v_2 can be generated via the so-called escape mechanism [31–35]. On the other hand, an explanation in terms of a hydrodynamic evolution of the system has also been put forward [36] (and criticised in [37]).

While viable explanations thus exist for the observation of non-vanishing v_2 of soft particles in small collision systems, the same is not true for the v_2 of high p_{\perp} particles found in such systems [38–40]. According to our current understanding, that would have to be generated by anisotropic energy loss, but the absence of jet quenching contradicts such an interpretation. However, the question

really remains a quantitative one, namely whether it is possible that a small amount of energy loss could generate a measurable high $p_{\perp} v_2$ while not leading to a measurable R_{AA} of hard particles or jets.

The present work aims to address precisely that question. To model the energy loss of hard partons, the JEWEL event generator is used. Usually one must make assumptions of what a medium looks like and how it should expand, which, in turn, adds uncertainties about the assumptions in the specific the medium model used. In order to reduce the dependence on the medium model, we take a different approach and look specifically into how many jet-medium interactions one needs in order to see the aforementioned effects. In practice, we actually look at the magnitude of the average number of interactions per jet particle times the squared Debye mass of the medium $\langle n_{\text{int}} \rangle \cdot (DM)^2$, as will be discussed in the later sections. Therefore, we perform this study using a simplified medium model and then, knowing the $\langle n_{\text{int}} \rangle \cdot (DM)^2$ needed to get effects of a given magnitude, we look into more realistic media.

2. JEWEL Monte Carlo Model

The Monte Carlo model JEWEL [41] simulates the QCD evolution of highly energetic partons produced in hard scattering processes in the presence of a background medium. It is based on PYTHIA 6.4 [42], which provides the hard scattering matrix elements, initial state parton shower and hadronisation. JEWEL has a virtuality ordered final state parton shower that is similar but not identical to the virtuality ordered parton shower in Pythia6. In vacuum this is an ordinary parton shower with the somewhat special feature that recoils from splittings are handled locally and in such a way that the algorithm never goes back to modify the kinematics of an earlier splitting. In the presence of a coloured medium, scattering off medium constituents can occur between the splittings generated by the parton shower. The scatterings are described by pQCD t -channel matrix elements regularised by the screening mass DM . If such a scattering is harder than the current parton shower scale it can reset the parton shower, re-starting it at the scale of the scattering. In this way, medium induced bremsstrahlung is effectively included and it is ensured that elastic and inelastic scattering occur with the leading-log correct relative rates. The Landau-Pomeranchuk-Migdal effect [43, 44] is included by allowing subsequent scatterings to act coherently if they fall within the formation time of the first splitting of a re-started parton shower. The momentum transfers are then added vectorially and the emission gets re-weighted with the inverse of the number of coherent momentum transfers. This procedure was shown to reproduce the BDMPS result in the eikonal limit [45]. Finally, re-starting the parton shower is only allowed when the first emission from the new shower has a shorter formation time than the current

emission from the old shower. The medium partons recoiling from an interaction with a hard parton can be kept in the event to provide a simple model of medium response. The parton shower partons, and where applicable also the recoils, are hadronised with the PYTHIA string hadronisation. JEWEL is largely agnostic about the background medium and it is therefore possible to interface with different medium models. However, it only simulates jets and medium response, but not the evolution of the bulk medium. Therefore, the events contain only particles that belong to the hard scattering and the parton showers or that have interacted with such a parton. For this study medium response is turned off in order to avoid complications in the interpretation of the results.

3. The small systems set-up

To address the puzzle of v_2 and R_{AA} in small systems we have used JEWEL with a *brick*-like medium. This medium model consists of a collection of gluons distributed in an ellipsoidal region of space over which the temperature and density are uniform. The geometry of this region is defined by two input parameters: the length of the long axis of that ellipse (or sphere when the eccentricity is zero) and its eccentricity. The density and temperature can also be specified by input parameters. The Debye mass, which regularises the scattering cross section and controls the hardness of the interactions, is related to the temperature in the default JEWEL setup. Here, we decouple it from the temperature and make it a free parameter allowing us to disentangle dependences.

All of the events (in medium or vacuum) used for the results in the upcoming sections are di-jet events at $\sqrt{s} = 5.02$ TeV generated with \hat{p}_{\perp} of the hard scattering between 50 and 500 GeV. In order to remove path length dependence (apart from the one coming from the geometry of the medium), we always generate the di-jets at the center of the brick.

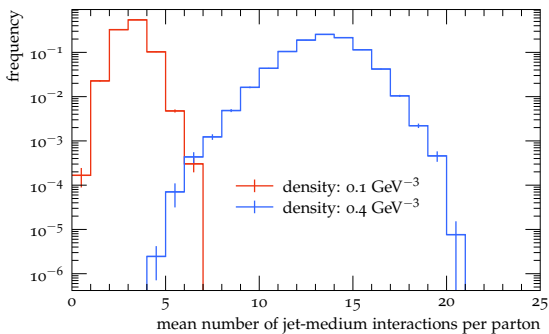
The two observables studied in the present work are R_{AA} of jets and v_2 of high p_{\perp} particles. To compute them (using the Rivet framework [46]) we consider all the final state hadrons with $p_{\perp} \geq 0.5$ GeV within a pseudo rapidity range of $|\eta| < 2.8$. Then, for R_{AA} , we reconstruct jets using the anti- k_{\perp} algorithm [47] with a radius of $R = 0.4$ and plot the p_{\perp} distributions of the reconstructed jets. To quantify the medium suppression, we integrate the spectra between 100 and 400 GeV and take the ratio of the integrals in medium and in vacuum.

As for the v_2 at high p_{\perp} , the default way to obtain it in small systems would be via correlations of high- p_{\perp} particles coming from the hard scattering with soft particles forming the background. This is done because the event plane in those systems is not well defined. However, the soft background is not available in JEWEL. We thus make use of equation 1 keeping in mind that, since the geometry of the brick is manually defined, the symmetry plane Ψ_2 is known. With that, and assuming all $v_{n>2} \approx 0$, we fit

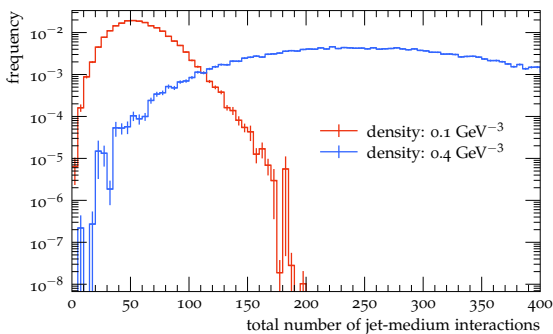
equation 1 to the normalised azimuthal angle distribution of all hadrons with $p_{\perp} \geq 2 \text{ GeV}$ and extract v_2 as a parameter of the fit. This is done event by event and the v_2 for a given set of parameters is the average for all the events in that set.

It is also important to clarify that, in order to understand the dependence of the observables of interest on the number of jet medium interactions, one must be careful not to introduce any biases related to the jet fragmentation pattern. Therefore, we calculate the observables of interest as a function of the *average* number of interactions at a given density. In other words, the number of interactions is tuned by changing the density while keeping the temperature, the system size, and geometry fixed. In this way, we calculate the observables on a sample of jets with different fragmentation patterns and different number of interactions with the medium. As seen in figure 1 the resulting distribution of the number of scatterings has a sizable width, but this is unavoidable since selecting jets based on the number of scatterings means selecting jets with a certain shape and fragmentation pattern.

We here fix the long axis of the brick to 1 fm and the temperature of the gluons to 200 MeV (this affects only the momentum distribution of gluons making up the background medium). The density, screening mass and eccentricity are varied.



(a)



(b)

Figure 1: Distributions of (a) mean number of interactions per hard parton (see text for definition) in an event; and (b) of total number of jet-medium interactions per d-jet for two different medium densities.

4. Results

We proceed with studying the R_{AA} dependence on the number of interactions. However, instead of plotting the results as a function of the number of jet-medium interactions, we plot them against the average number of interactions per parton ($\langle n_{\text{int}} \rangle$) times the square of the Debye mass (DM), which is a proxy for the average momentum squared exchanged per parton between jet and medium. This is done because the DM controls how hard the interactions are, which strongly affects the energy loss per interaction and, consequently, the R_{AA} .¹ To demonstrate the approximate scaling with $\langle n_{\text{int}} \rangle \cdot (\text{DM})^2$, we calculate R_{AA} and v_2 as a function of $\langle n_{\text{int}} \rangle \cdot (\text{DM})^2$ for two different values of the DM, as seen in figure 2. The number of interactions per parton is calculated taking into account the entire (splitting) history of the partons. At the end of the partonic phase we find all partons present at that stage. We then follow each parton backwards through the evolution counting the number of scatterings. When a splitting is reached we continue with the mother parton. In this way all scatterings in the history of the parton are counted. The resulting distributions of number of scatterings are shown in figure 1.

Figure 2 shows that both R_{AA} and v_2 scale almost linearly with $\langle n_{\text{int}} \rangle \cdot (\text{DM})^2$. The dot dashed lines in figure 2(a) show the point at which the R_{AA} goes below 0.9, which is around the value of R_{AA} that can be reliably measured. We extract the value of $\langle n_{\text{int}} \rangle \cdot (\text{DM})^2$ at which this happens from a linear fit to the R_{AA} values and obtain 3.1(1) GeV^2 , corresponding to 12 interactions per parton in the case of $\text{DM}=0.55 \text{ GeV}$ and around 8 interactions for $\text{DM}=0.68 \text{ GeV}$. These numbers correspond to a total of around 100 to 150 interactions in the di-jet event. This is counting all scatterings of partons belonging to the hard partonic system, including those of partons that end up outside the reconstructed jets.

On the other hand, figure 2(b) shows the result of v_2 divided by the eccentricity (ϵ_2) of the brick (we find that v_2 is proportional to ϵ_2). The eccentricity is calculated from the position of the scatterings using $\epsilon_2 = \langle y^2 - x^2 \rangle / \langle x^2 + y^2 \rangle$. In figure 2(b), the dot dashed lines show the value of v_2 at the same point where a 10% effect in R_{AA} was observed in figure 2(a). That is, for $\langle n_{\text{int}} \rangle \cdot (\text{DM})^2 = 3.1 \text{ GeV}^2$, $v_2 / \epsilon_2 = 0.033(1)$, which corresponds to $v_2 = 0.0099(3)$ for an intermediate eccentricity of 0.3. It should be noted that, when computing v_2 in the way described in section 3, i.e., relative to the symmetry plane, it should be considered as an underestimate of the values obtained in experiments from two particle correlations. The latter is generally larger than the former, for instance, because it responds differently to fluctuations. We, thus, do not see our results as a contradiction to the measurements. Nonetheless, these results indicate that once the system

¹In a single scattering the energy loss of the energetic parton scales approximately as $(\text{DM})^2$.

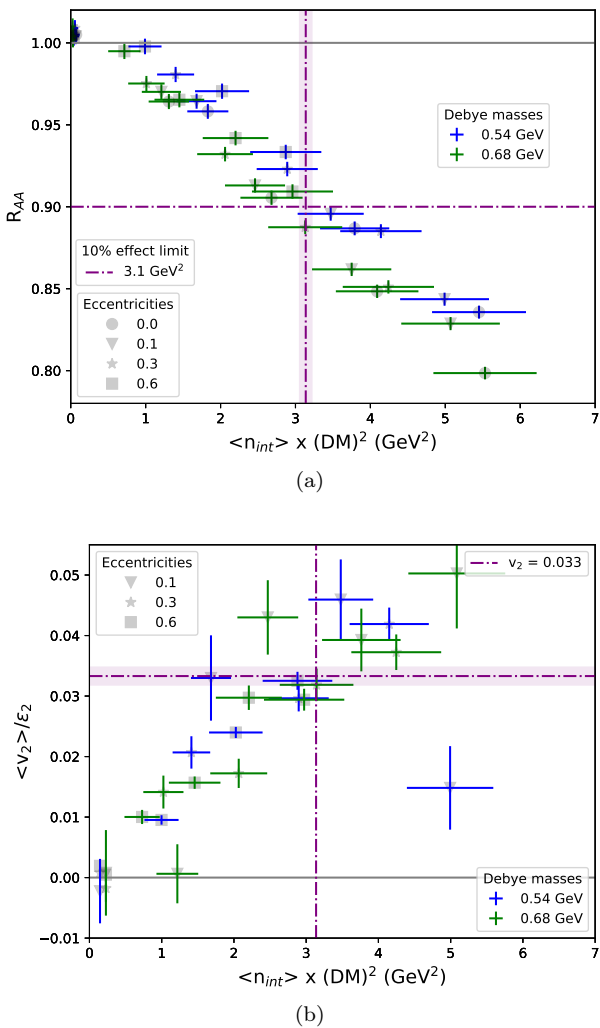


Figure 2: (a) R_{AA} and (b) v_2 results also as a function of $\langle n_{int} \rangle \cdot (DM)^2$.

has interacted enough to produce a v_2 of high p_{\perp} particles, R_{AA} should also show substantial suppression.

We also verified the range of validity of the linear scaling with $\langle n_{int} \rangle \cdot (DM)^2$. Figure 3(a) shows the R_{AA} as a function of brick radius for different parameter settings with the same $\langle n_{int} \rangle \cdot (DM)^2$. It becomes clear that, as the size of the medium increases, the same value of $\langle n_{int} \rangle \cdot (DM)^2$ produces more suppression when compared with the smaller medium. This is most pronounced for higher values of the Debye mass. In JEWEL the amount of medium induced radiation depends rather strongly on the Debye mass, because it is much easier for harder scatterings to initiate medium induced emissions. It is also easier for a scattering to induce an emission at later times, when emissions from the parton shower of the initial hard scattering tend to have longer formation times. This leads to an increase of medium induced emissions per scattering as a function of system size as seen in figure 3(b). Thus, when the inelastic interactions are turned off (i.e. there is

only elastic scattering), this suppression is not as important. This indicates that the breaking of this scaling is largely due to a sizable contribution from inelastic interactions. It is worth noting that, in the medium, angular ordering is not imposed between two splittings if an interaction has taken place between them. Therefore, even the points with only elastic interactions are expected to have more splittings than the jets in vacuum. As for the remaining difference, it is accounted for by medium induced emissions. Therefore, the plots in figure 3(b) indicate that inelastic energy loss does not follow the scaling, and, in small systems, where the scaling approximately holds, energy loss is mainly driven by elastic interactions. Figure 3 also shows that, while inelastic energy loss is an important factor for departures from scaling, there is an effect even in the absence of inelastic scattering. This is because, even for elastic scattering, the time at which a scattering occurs is not completely irrelevant (as assumed by the scaling). At early times the partons did not have time to radiate much yet and therefore the average parton energy is higher than at later times. A higher parton energy implies a smaller energy loss for the same momentum transfer and an early scattering thus leads to a somewhat smaller energy loss than a later one. Also, early scatterings contribute less to broadening, which transports energy out of the jet cone. This is so because a scattering of a parton early in the branching history tends to deflect the whole jet rather than individual constituents of the jet.

To confirm that the earlier scatterings contribute less to R_{AA} than the later ones, we have taken the spherical brick with radius of 1 fm and split it into two: one smaller spherical brick of radius 0.5 fm and one hollow spherical brick of radius 1.0 fm which has no medium within the first 0.5 fm radius. Both of them have the same density (0.1 or 0.2 GeV^{-3}) and Debye mass (0.68 GeV). The results are shown in Table 1 and one can see that, for very close values of $\langle n_{int} \rangle \cdot (DM)^2$, the later interactions lead to a stronger suppression.

Density (GeV^{-3})	R_{in} (fm)	R_{out} (fm)	$\langle n_{int} \rangle \cdot (DM)^2$ (GeV^2)	R_{AA}
0.1	0.0	0.5	1.6(3)	0.974(5)
0.1	0.5	1.0	1.7(3)	0.926(4)
0.2	0.0	0.5	3.4(5)	0.916(4)
0.2	0.5	1.0	3.6(5)	0.841(4)

Table 1: $\langle n_{int} \rangle \cdot (DM)^2$ and R_{AA} in events where there is a medium between a radius R_{in} and a radius R_{out} .

Finally, we also generated events using a somewhat more realistic medium model, which accounts for longitudinal expansion and has a temperature profile. This is the simplistic medium model that comes with JEWEL [41]. We want to stress that this is by no means a realistic model, and, in particular, it is expected to perform poorly for small systems [48]. The motivation for using it here is rather to have a model that is qualitatively different from

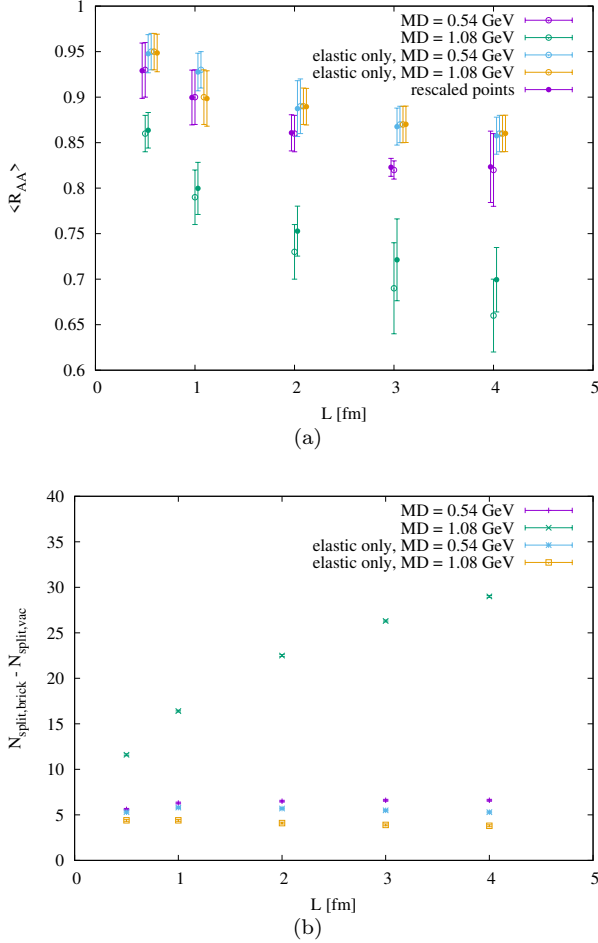


Figure 3: (a) R_{AA} as a function of brick radius for points with similar $\langle n_{\text{int}} \rangle \cdot (\text{DM})^2$. Since the points have slightly different $\langle n_{\text{int}} \rangle \cdot (\text{DM})^2$ we have rescaled R_{AA} to a common $\langle n_{\text{int}} \rangle \cdot (\text{DM})^2 = 3.5 \text{ GeV}^2$ assuming a linear dependence of R_{AA} on $\langle n_{\text{int}} \rangle \cdot (\text{DM})^2$. (b) Difference in number of splittings between the medium simulations and the corresponding vacuum corresponding to the points in (a).

the brick medium. We generated events for HeHe and deuteron-deuteron collisions, which yield values of $\langle n_{\text{int}} \rangle \cdot (\text{DM})^2$ that are similar to those studied with the brick medium. The initial temperatures were obtained by scaling the energy densities from T_RENTo [49], except for the higher values for the 0-10% centrality classes, which were added to obtain higher values of $\langle n_{\text{int}} \rangle \cdot (\text{DM})^2$. For the initialisation time $\tau_i = 0.4 \text{ fm}$ was used in all cases. It should be noted that now the screening mass varies with temperature throughout the evolution and therefore instead of $\langle n_{\text{int}} \rangle \cdot (\text{DM})^2$ we compute for each parton the sum of the actual values of the squared screening mass for each scattering, denoted as $\langle \sum \text{DM}^2 \rangle$ (for the brick medium $\langle n_{\text{int}} \rangle \cdot (\text{DM})^2 = \langle \sum \text{DM}^2 \rangle$). Figure 4 shows that with the expanding medium R_{AA} falls off more steeply with $\langle \sum \text{DM}^2 \rangle$ than with the brick medium. This divergence from the result in figure 2(a) could be due to the fact that the medium model used was not tailored for application in small systems. In particular, it has a linear increase

of the temperature until the initial proper time τ_i (after which longitudinal expansion leads to a decreasing temperature). For the results shown here τ_i is a large fraction of the total size and lifetime of a small collision system. Most scatterings, thus, occur at relatively late times and figure 3 indicates that this is expected to lead to a stronger suppression. Nonetheless, figure 4 also shows a scaling of the R_{AA} with $\langle \sum \text{DM}^2 \rangle$, thus supporting the findings with the brick.

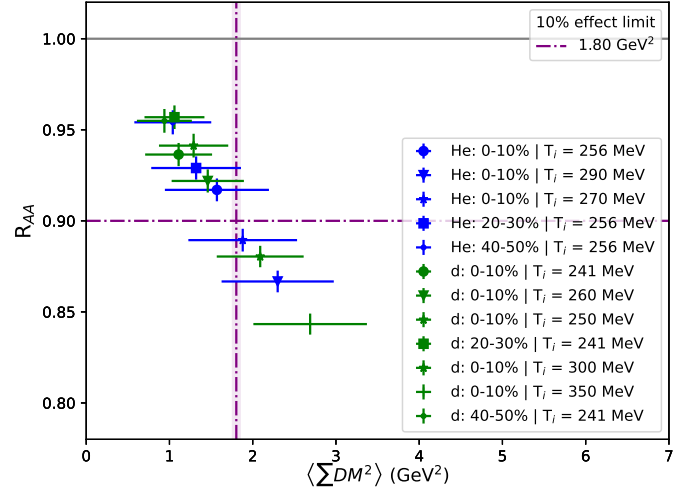


Figure 4: R_{AA} as a function of $\langle \sum \text{DM}^2 \rangle$ for the expanding medium, where DM is allowed to vary and $\langle \sum \text{DM}^2 \rangle$ stands for the average sum of DM^2 for each interaction per parton.

5. Conclusions

We have studied how the number of jet-medium interactions affects different jet quenching observables. The first important observation is that the result is largely dependent on the screening mass of the medium and, in fact, R_{AA} and v_2 scale approximately with $\langle n_{\text{int}} \rangle \cdot (\text{DM})^2$. Figure 2 shows how these observables depend on $\langle n_{\text{int}} \rangle \cdot (\text{DM})^2$ and that at $3.1(1) \text{ GeV}^2$ a 10% effect is observed in R_{AA} . At the same point, and for the intermediate eccentricity studied ($\epsilon_2 = 0.3$), $v_2 = 0.0099(3)$. This value of $\langle n_{\text{int}} \rangle \cdot (\text{DM})^2$ corresponds to a number between 8 and 12 interactions per parton in the range of Debye masses studied. This means that, in total, around 100 – 150 interactions between the fragmenting partonic system (per event for pure QCD hard scatterings) and medium particles are required to obtain an observable R_{AA} in small systems. But we have also studied the validity of this scaling behavior and figure 3 shows that it breaks down for larger system sizes. It also shows that, when the system size is small, the energy loss happens mainly through elastic scatterings. The reasons for departure from scaling are radiative energy loss, which does not follow the scaling and in JEWEL is more important at later times, and the

fact that elastic scattering is more effective for jet quenching when it occurs at later times. Finally, we looked at a more realistic medium model and saw that R_{AA} shows a stronger dependence on $\langle \sum DM^2 \rangle$ than the brick medium. This shows that there is a scaling behavior of R_{AA} and v_2 with the number of scatterings and the square of the Debye mass, but the size of the system and the spatio-temporal distribution of scatterings also plays a role.

Acknowledgments

We would like to thank Alice Ohlson for enlightening discussions. This study is part of a project that has received funding from the European Research Council (ERC) under the European Union's Horizon 2020 research and innovation programme (Grant agreement No. 803183, collectiveQCD). JGM was partly supported ERC under the European Union's Horizon 2020 research and innovation programme (Grant agreement No. 835105, YoctoLHC).

References

- [1] James Daniel Bjorken. Energy loss of energetic partons in quark - gluon plasma: Possible extinction of high p(t) jets in hadron - hadron collisions. *FERMILAB-PUB*, 82, 1982.
- [2] R. Baier, Yu.L. Dokshitzer, A.H. Mueller, S. Peigné, and D. Schiff. Radiative energy loss of high energy quarks and gluons in a finite-volume quark-gluon plasma. *Nuclear Physics B*, 483(1):291–320, 1997.
- [3] Urs Achim Wiedemann. Jet Quenching in Heavy Ion Collisions. pages 521–562, 2010.
- [4] A. Majumder and M. Van Leeuwen. The Theory and Phenomenology of Perturbative QCD Based Jet Quenching. *Prog. Part. Nucl. Phys.*, 66:41–92, 2011.
- [5] Yacine Mehtar-Tani, Jose Guilherme Milhano, and Konrad Tywoniuk. Jet physics in heavy-ion collisions. *Int. J. Mod. Phys. A*, 28:1340013, 2013.
- [6] Guang-You Qin and Xin-Nian Wang. Jet quenching in high-energy heavy-ion collisions. *Int. J. Mod. Phys. E*, 24(11):1530014, 2015.
- [7] Liliana Apolinário, Yen-Jie Lee, and Michael Winn. Heavy quarks and jets as probes of the QGP. *Prog. Part. Nucl. Phys.*, 127:103990, 2022.
- [8] K. Aamodt and et al. Suppression of charged particle production at large transverse momentum in central pbpb collisions at $\sqrt{s_{NN}}=2.76$ tev. *Physics Letters B*, 696(1):30–39, 2011.
- [9] C. Adler and et al. Centrality dependence of high- p_T hadron suppression in Au + Au collisions at $\sqrt{s_{NN}} = 130$ GeV. *Phys. Rev. Lett.*, 89:202301, Oct 2002.
- [10] Megan Connors, Christine Nattrass, Rosi Reed, and Sevil Salur. Jet measurements in heavy ion physics. *Rev. Mod. Phys.*, 90:025005, 2018.
- [11] Leticia Cunqueiro and Anne M. Sickles. Studying the QGP with Jets at the LHC and RHIC. *Prog. Part. Nucl. Phys.*, 124:103940, 2022.
- [12] J. Adams and et al. Evidence from $d + Au$ measurements for final-state suppression of high- p_T hadrons in Au + Au collisions at rhic. *Phys. Rev. Lett.*, 91:072304, Aug 2003.
- [13] B. Abelev and et al. Transverse momentum distribution and nuclear modification factor of charged particles in $p+Pb$ collisions at $\sqrt{s_{NN}}=5.02$ TeV. *Phys. Rev. Lett.*, 110:082302, Feb 2013.
- [14] Jaroslav Adam et al. Measurement of charged jet production cross sections and nuclear modification in p-pb collisions at $\sqrt{s_{NN}} = 5.02$ tev. *Phys. Lett. B*, 749:68–81, 2015.
- [15] Vardan Khachatryan et al. Transverse momentum spectra of inclusive b jets in pPb collisions at $\sqrt{s_{NN}} = 5.02$ TeV. *Phys. Lett. B*, 754:59, 2016.
- [16] Vardan Khachatryan et al. Measurement of inclusive jet production and nuclear modifications in pPb collisions at $\sqrt{s_{NN}} = 5.02$ TeV. *Eur. Phys. J. C*, 76(7):372, 2016.
- [17] Shreyasi Acharya et al. Measurement of inclusive charged-particle b-jet production in pp and p-pb collisions at $\sqrt{s_{NN}} = 5.02$ tev. *JHEP*, 01:178, 2022.
- [18] Georges Aad et al. Strong Constraints on Jet Quenching in Centrality-Dependent p+Pb Collisions at 5.02 TeV from ATLAS. *Phys. Rev. Lett.*, 131(7):072301, 2023.
- [19] Shreyasi Acharya et al. Search for jet quenching effects in high-multiplicity pp collisions at $\sqrt{s} = 13$ TeV via di-jet acoplanarity. *JHEP*, 05:229, 2024.
- [20] Georges Aad et al. Centrality and rapidity dependence of inclusive jet production in $\sqrt{s_{NN}} = 5.02$ TeV proton-lead collisions with the ATLAS detector. *Phys. Lett.*, B748:392–413, 2015.
- [21] Vardan Khachatryan et al. Nuclear Effects on the Transverse Momentum Spectra of Charged Particles in pPb Collisions at $\sqrt{s_{NN}} = 5.02$ TeV. *Eur. Phys. J.*, C75(5):237, 2015.
- [22] Jaroslav Adam et al. Centrality dependence of charged jet production in p-Pb collisions at $\sqrt{s_{NN}} = 5.02$ TeV. *Eur. Phys. J.*, C76(5):271, 2016.
- [23] Jaroslav Adam et al. Multiplicity dependence of charged pion, kaon, and (anti)proton production at large transverse momentum in p-Pb collisions at $\sqrt{s_{NN}} = 5.02$ TeV. *Phys. Lett.*, B760:720–735, 2016.
- [24] B. Abelev and et al. Multiparticle azimuthal correlations in p-pb and pb-pb collisions at the cern large hadron collider. *Phys. Rev. C*, 90:054901, Nov 2014.
- [25] B. Abelev and et al. Elliptic flow of identified hadrons in Pb-Pb collisions at $\sqrt{s_{NN}} = 2.76$ TeV. *Journal of High Energy Physics*, 190:1029–8479, 2015.
- [26] Xiaoning Wang. Measurements of the azimuthal anisotropy of jets and high- p_T charged particles in Pb+Pb collisions with the ATLAS detector. *PoS, HardProbes2023*:159, 2024.
- [27] G. Agakishiev et al. Energy and system-size dependence of two- and four-particle v_2 measurements in heavy-ion collisions at RHIC and their implications on flow fluctuations and non-flow. *Phys. Rev. C*, 86:014904, 2012.
- [28] Vladimir Korotkikh. Elliptic flow studies in heavy-ion collisions using the CMS detector at the LHC. 12 2010.
- [29] A. M. Sirunyan and et al. Observation of correlated azimuthal anisotropy fourier harmonics in pp and $p + Pb$ collisions at the lhc. *Phys. Rev. Lett.*, 120:092301, Feb 2018.
- [30] V. Khachatryan and et al. Evidence for collective multiparticle correlations in p-Pb collisions. *Phys. Rev. Lett.*, 115:012301, Jun 2015.
- [31] Aleks Kurkela, Urs Achim Wiedemann, and Bin Wu. Nearly isentropic flow at sizeable η/s . *Phys. Lett. B*, 783:274–279, 2018.
- [32] Victor E. Ambrus, S. Schlichting, and C. Werthmann. Development of transverse flow at small and large opacities in conformal kinetic theory. *Phys. Rev. D*, 105(1):014031, 2022.
- [33] Liang He, Terrence Edmonds, Zi-Wei Lin, Feng Liu, Denes Molnar, and Fuqiang Wang. Anisotropic parton escape is the dominant source of azimuthal anisotropy in transport models. *Phys. Lett. B*, 753:506–510, 2016.
- [34] Denes Molnar. How AMPT generates large elliptic flow with small cross sections. 6 2019.
- [35] Aleks Kurkela, Aleksas Mazeliauskas, and Robin Törnkvist. Collective flow in single-hit QCD kinetic theory. *JHEP*, 11:216, 2021.
- [36] Ryan D. Weller and Paul Romatschke. One fluid to rule them all: viscous hydrodynamic description of event-by-event central p+p, p+Pb and Pb+Pb collisions at $\sqrt{s} = 5.02$ TeV. *Phys. Lett. B*, 774:351–356, 2017.
- [37] You Zhou, Wenbin Zhao, Koichi Murase, and Huichao Song. One fluid might not rule them all. *Nucl. Phys. A*, 1005:121908, 2021.
- [38] Georges Aad et al. Transverse momentum and process depen-

- dent azimuthal anisotropies in $\sqrt{s_{\text{NN}}} = 8.16$ TeV p +Pb collisions with the ATLAS detector. *Eur. Phys. J. C*, 80(1):73, 2020.
- [39] Shreyasi Acharya et al. Azimuthal anisotropy of jet particles in p-Pb and Pb-Pb collisions at $\sqrt{s_{\text{NN}}} = 5.02$ TeV. *JHEP*, 08:234, 2024.
- [40] Elliptic anisotropy at high p_{T} in pPb collisions using subevent cumulants. Technical report, CERN, Geneva, 2024.
- [41] Korinna C. Zapp, Frank Krauss, and Urs A. Wiedemann. A perturbative framework for jet quenching. *JHEP*, 1303:080, 2013.
- [42] Torbjorn Sjostrand, Stephen Mrenna, and Peter Skands. PYTHIA 6.4 physics and manual. *JHEP*, 05:026, 2006.
- [43] L. D. Landau and I. Pomeranchuk. Electron cascade process at very high-energies. *Dokl. Akad. Nauk Ser. Fiz.*, 92:735–738, 1953.
- [44] Arkady B. Migdal. Bremsstrahlung and pair production in condensed media at high-energies. *Phys. Rev.*, 103:1811–1820, 1956.
- [45] Korinna Christine Zapp, Johanna Stachel, and Urs Achim Wiedemann. A local Monte Carlo framework for coherent QCD parton energy loss. *JHEP*, 07:118, 2011.
- [46] Christian Bierlich et al. Robust Independent Validation of Experiment and Theory: Rivet version 3. *SciPost Phys.*, 8:026, 2020.
- [47] Matteo Cacciari, Gavin P. Salam, and Gregory Soyez. The anti- k_t jet clustering algorithm. *JHEP*, 04:063, 2008.
- [48] Korinna C. Zapp. Geometrical aspects of jet quenching in JEWEL. *Phys. Lett. B*, 735:157–163, 2014.
- [49] J. Scott Moreland, Jonah E. Bernhard, and Steffen A. Bass. Alternative ansatz to wounded nucleon and binary collision scaling in high-energy nuclear collisions. *Phys. Rev. C*, 92(1):011901, 2015.